Rethinking Classical Crystal Growth Models through Molecular Scale Insights: Consequences of Kink-Limited Kinetics

ARTICLE *in* CRYSTAL GROWTH & DESIGN · DECEMBER 2009

Impact Factor: 4.89 · DOI: 10.1021/cg900543g

8 AUTHORS, INCLUDING:

Laura Wasylenki
Indiana University Bloomington
43 PUBLICATIONS **790** CITATIONS
SEE PROFILE

George H. Gilmer
Colorado School of Mines
221 PUBLICATIONS **8,380** CITATIONS
SEE PROFILE

DOI: 10.1021/cg900543g

CRYSTAL GROWTH & DESIGN Article

2009, Vol. 9
5135–5144

Rethinking Classical Crystal Growth Models through Molecular Scale Insights: Consequences of Kink-Limited Kinetics

J. J. De Yoreo,*,† L. A. Zepeda-Ruiz,‡ R. W. Friddle,†,‡ S. R. Qiu,‡ L. E Wasylenki,§,# A. A. Chernov,‡ G. H. Gilmer,‡ and P. M. Dove*,§

†*Molecular Foundry, Lawrence Berkeley Laboratory, Berkeley, California 94720,* ‡*Department of Physical and Life Sciences, Lawrence Livermore National Laboratory, Livermore, California 94551, and* §*Department of Geosciences, Virginia Tech, Blacksburg, Virginia 24061.* #*Current address: Department of Geological Sciences, Arizona State University, Tempe, Arizona 85287*

Received May 20, 2009; Revised Manuscript Received September 28, 2009

ABSTRACT: The classical terrace-ledge-kink model of crystal growth is widely used to interpret mineral formation in biological and geological systems. A key assumption underlying application of the model is that thermal fluctuations of steps are sufficiently rapid to produce an abundance of kink sites for attachment of growth units. High-resolution in situ atomic force microscopy (AFM) studies and kinetic Monte Carlo simulations of step-edge structure and dynamics show this physical picture to be invalid for the common mineral calcite whose steps exhibit low kink density and weak step edge fluctuations. As a consequence, interactions of impurities with calcite step edges cannot be interpreted with traditional thermodynamic models based on minimization of the Gibbs free energy. Instead, impurity-step interactions follow a different mechanism determined by the kinetics of attachment and detachment. Step advance is unimpeded when the creation of new kinks by attachment of growth units to the step outpaces binding of impurities to the newly created kinks. This kink-limited model offers a plausible explanation for reports of "kinetic disequilibrium" of trace element signatures. Moreover, because kink density is tied to crystal solubility, these findings argue for a theory based on weak fluctuations to interpret growth of many common crystalline phases of importance in geochemical, biological, and technological settings.

Introduction

The mechanistic foundation for interpreting the growth of crystals in near-surface geological and biological settings has generally been provided by the classic atomic-scale terrace-ledge-kink (TLK) model. The theory for growth by this process, as formulated by Burton, Cabrera, and Frank (BCF)[1] more than half a century ago, has been widely applied to diverse systems in experiments far removed from the atomic scale. The physical model describes propagation of a crystal facet by attachment of growth units onto step edges. Final attachment to the growing crystal occurs predominantly at locations known as kink sites, where the atomic row that defines the step edge is incomplete (Figure 1a). Kinks are created via random attachments and detachments of growth units to and from this atomic row and are unique sites because the chemical potential per molecule of a growth unit at a kink is equal to that of the crystal itself.[2] Close to equilibrium, this random exchange between crystal and solution is described by classical statistical mechanics and exhibits characteristics associated with minimizing the Gibbs free energy.

A crucial underlying assumption commonly associated with applications of the BCF model to these types of systems is that the steps obey the fluctuation dissipation theorem (FDT)[3] of thermodynamics. That is, even as the system is moved away from equilibrium, the rate of kink formation through fluctuations is fast enough to continue describing it by minimizing the Gibbs free energy. This implies that the rate of kink formation is faster than the rate at which left- and right-facing kinks meet and annihilate one another as the step advances (Figure 1a). As a consequence, step propagation is limited only by the kinetics of solute attachment and detachment at kinks, and finite step segments exhibit cooperativity that allows their thermodynamic state to be described by the Gibbs−Thomson Law (GTL)[4] relating the true thermodynamic driving force to the finite length of the step. The GTL leads directly to many of the BCF predictions used to interpret mineral growth and dissolution experiments, such as those pertaining to step morphology and growth rate, as well as the effect of impurities[5] on these two defining features.

When step edge fluctuations are strong enough to continuously provide a large reservoir of kink sites to the step edge, this classical model works well.[6,7] But the crystal systems that motivated development of the BCF model within the limits of validity of the Gibbs−Thomson law — and to which it was initially applied — were those grown from high-temperature melts, through vapor deposition, or from highly soluble salts where the FDT appears to be applicable.[8] Prior estimates of kink density at equilibrium for such systems showed that they were sufficiently high to warrant this approach.[9] However, in the ensuing years, numerous crystal systems have been found to have weak step fluctuations and, as a result, low kink densities. The Si and Ge (100) surfaces at sufficiently low temperatures present the canonical examples. Surface reconstruction leads to dimer row formation such that steps parallel to the rows have interkink distances of many 10's of lattice sites.[10] Moreover, some researchers have presented theoretical analyses calling into question the assumption that step fluctuations are rapid even during solution crystallization and especially in low temperature environments.[11,12] For example, Nielsen[13] included a supersaturation-dependent kink density to explain parabolic growth rate laws during electrolyte

*To whom correspondence should be addressed. E-mail: jjdeyoreo@lbl.gov; dove@vt.edu.

Published on Web 11/11/2009

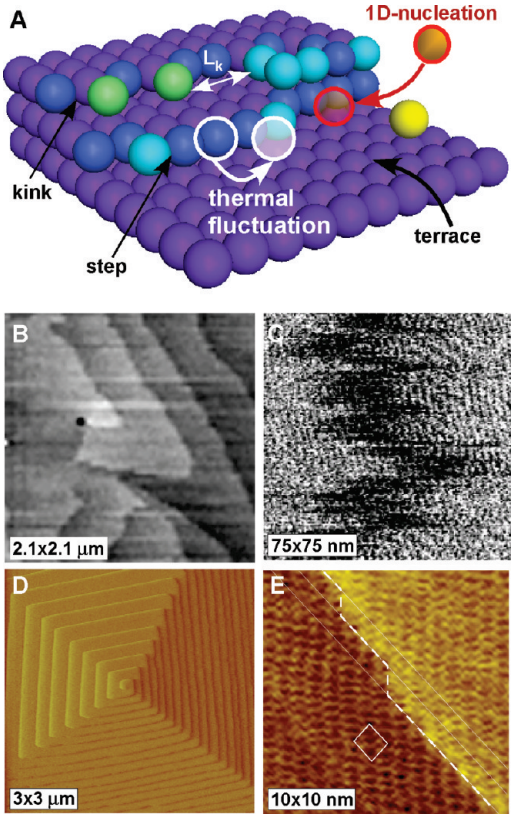

Figure 1. (A) Schematic illustrating terrace, step, and kinks on crystal surface. Kinks are created either via movements of molecule on the step edge (thermal fluctuations) or attachment of new solute molecules from solution (1D nucleation). The step advances because addition of molecules to right- and left-facing kinks leads to their lateral movement and eventual annihilation. (B−E) AFM images showing steps generated near equilibrium at spiral growth hillocks on (B) the KDP (101) face, (C) one of the two equivalent steps on the KDP (010) face[29], (D) the calcite (104) face, and (E) one of the two equivalent obtuse steps on the calcite (104) face at low (B, D) and high (C, E) resolution. (See ref 23 for definition of calcite obtuse and acute steps.) Steps on KDP fluctuate by approximately 35 nm over a length of 75 nm and have high kink density while steps on calcite exhibit little fluctuation and few kinks.

crystallization. Zhang and Nancollas[11] pointed out that, for sparingly soluble crystals at low temperatures, equilibrium kink density should be low and kink formation should be an important contributor to the kinetics of step growth. More recently, Cuppen et al.[14] used kinetic Monte Carlo methods to extensively examine both the dependence of kink density on crystal structure, bond energies and supersaturation, and the consequences for step propagation kinetics, both for Kossel[14] and non-Kossel[15] crystal lattices. Nonetheless, the BCF model in the limit where the Gibbs−Thomson law is valid has continued to be used almost exclusively to interpret experimental studies of mineral growth and dissolution as well as the effects of impurities. Its predictions have even been used to confer mechanistic significance to parameters determined from bulk crystallization experiments, such as the power law exponents of rate equations.

Over the past decade, the ability to image mineral surfaces during growth from solutions using in situ atomic force microscopy (AFM) has enabled researchers to directly observe atomic step behavior. A critical examination of these studies on crystals of both proteins[16−18] and common mineral or biomineral phases such as calcite,[19−24] barite,[25] and brushite[17] has raised serious doubts that growth of such materials can fully be explained by a theory that assumes step fluctuations are rapid. For example, the initial generation and movement of steps near dislocation sources on these crystals violates predictions based on the Gibbs−Thomson law, and the behavior of converging steps provides strong evidence that step propagation is, in fact, limited by the availability of kinks. Thus, significant deviations from the classical picture of rapid fluctuations appear to occur within relative supersaturations of only a few percent, a regime that is ubiquitous in mineral systems.

In what follows, we use true atomic scale AFM imaging to present direct evidence that calcite kink generation near equilibrium is too slow to satisfy the assumptions of strong step fluctuations. We then demonstrate that application of the Gibbs−Thomson law dramatically fails to predict the influence of the simple inorganic impurity, Sr^{2+}, on calcite growth. We couple these experimental data with findings from kinetic Monte Carlo (kMC) simulations that reveal the underlying reason why systems that violate the fundamental assumption of strong step fluctuations should exhibit the behavior observed for calcite. Because, as we discuss below, fluctuation rates should generally scale with crystal solubility, the findings provide strong evidence for the earlier argument that growth of sparingly soluble crystals is limited by the availability of kinks,[11] a conclusion that has significant implications for the interpretation of impurity signatures in calcite and other minerals. These results cast doubt on the applicability of versions of the TLK model based on the validity of the Gibbs−Thomson law to many common crystalline phases — particularly minerals that are stable in the biosphere — and call for a revised formalism to describe mineral growth and impurity interactions that account for weak step fluctuations.

Analysis and Discussion

Relationship between Step Structure and Energy Barrier to Kink Formation. Under conditions where the surface energy per unit area on a singular crystal facet is greater than or comparable to the thermal energy kT, the facet is below the roughening transition temperature. That is, it is atomically flat. Under this condition, when a crystal facet is slightly inclined with respect to the singular direction, it is comprised of steps separated by atomically flat terraces (Figure 1a). At equilibrium, fluctuations in the occupation number of the lattice rows along the step edges due to thermally activated detachment and attachment events are the source of kinks. When the kink creation energy ε is less than kT, where k is the Boltzmann constant and T is absolute temperature, at equilibrium, eventually the average spacing between kinks $L_k \sim (b/2)\exp(\varepsilon/kT)$ will be nearly equal to the lattice spacing ($b/L_k \sim 1/2$ where b is the lattice spacing) [1]. The condition, $\varepsilon < kT$ is thus the limit of rough steps at equilibrium.[8] (In the limit of $\varepsilon \ll kT$, the step free energy becomes negative so that the step cannot exist, meaning that the crystal facet overcomes the roughening transition and becomes atomically rough.)

The kink energy can be estimated by the step riser energy per growth unit. So defined, it decreases linearly with the logarithm of solubility.[26] Consequently, following the concepts reiterated above, the less soluble the crystal is, the lower the equilibrium kink density will be. Qualitatively, the relationship between the equilibrium kink density and solubility may be understood in terms of the dynamics of a step,

as follows. The kink energy ε is the minimal work required to create a kink. Suppose one creates two kinks of opposite signs by transferring to solution several growth units from the row on the edge of a straight step. The net minimal work of this transfer equals the sum of the work spent to break bonds between the growth units and the lattice and that spent to break the bonds between themselves, minus the work that is gained back when these units and the step riser are solvated and reconstructed to their equilibrium configuration. The difference between the work spent and returned, minus the dissolution enthalpy, times the number of particles transferred is the energy of the two newly created kinks. Because the work returned due to solvation scales with the solute−solvent affinity, that is, the solubility, lower solubility should be associated with higher kink energy, which results in smoother steps.

Unlike the equilibrium kink density discussed above, the fluctuation rate is related to the kinetic barriers and frequencies for attachment and detachment of the growth units. These parameters enter kinetic coefficients that are more poorly known than solubilities. However, following the general wisdom of chemical kinetics that a smaller bond energy results in a lower kinetic barrier to form or to rupture the bond in a chemical reaction, one typically assumes that, for $\varepsilon < kT$, crystal−solution exchange by species is more rapid than in the case of high kink energy. Therefore, the time period required for this equilibrium kink density to be reached is smaller. That is, the FDT applies even at high growth rates as long as the kink generation rate still exceeds the mutual kink annihilation rate. In this regime, the kink reservoir is large and kinks are always available for solute attachment and detachment. Because attachment and detachment events are statistically independent, the rate of step advancement v exhibits linear kinetics. That is, it is linearly proportional to the difference between the actual and equilibrium concentrations of the solute $C-C_e$ according to

$$v = \beta\omega(C - C_e) \quad (1)$$

where β is the kinetic coefficient and ω is the volume per molecule in the solid.

A good example of a material with a low energy barrier to kink formation is shown by AFM images of KH_2PO_4 (KDP) (Figure 1b,d), a highly soluble salt ($C_e \sim 3$ M) for which the linear dependence of v on $C - C_e$ is well established.[27,28] Even at a resolution low enough to see multiple turns of a dislocation spiral, the roughness of the step edges is visible (Figure 1b). In higher resolution images (Figure 1d), the extreme fluctuations of the step present at equilibrium ($C = C_e$) are well-resolved.[29] Over a length of 75 nm, the step itself wanders back and forth some 25 nm from its average position.

In contrast, calcite, whose solubility is ~10 000 times less than that of KDP, exhibits smooth step edges that essentially do not wander from their average crystallographic orientations at equilibrium (Figure 1c,e). From higher resolution images like that in Figure 1e, we estimate the average spacing between kink sites to be about six lattice sites, which gives a kink density below the rough limit discussed above. In addition, as Figure 2 shows, time traces of a single location along a step reveal that the fluctuations in the position of the step do not exceed ± 1 lattice site over long periods of time. In other words, not only is the equilibrium kink density below that expected for rough steps, but the rate at which new kinks are generated by step fluctuations is low on the typical time scale of growth. This is consistent with kinetic Monte Carlo simulations of step speed[14] for $\varepsilon > kT$, as well as measurements made on calcite that show a nonlinear dependence on concentration.[24] We conclude that step fluctuations for calcite are too weak for the FDT to apply and interpretation of growth or dissolution experiments must assume that the creation of kinks is the rate-limiting step in the process.

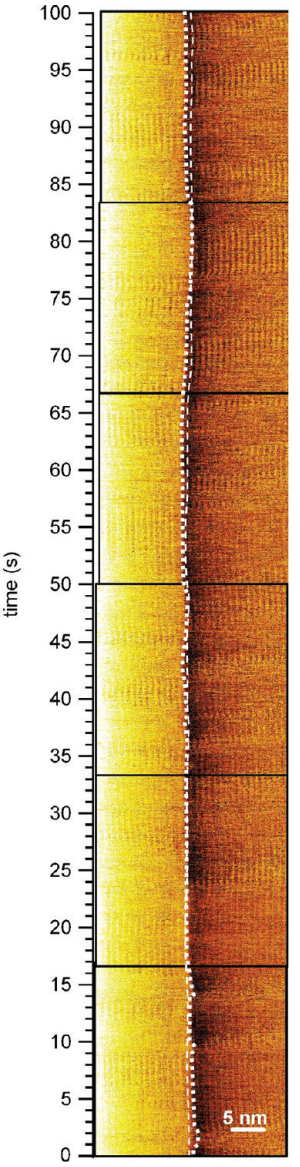

Figure 2. Continuous trace across a single location along an obtuse step on the calcite (104) face, obtained by scanning the AFM tip perpendicular to the step and disabling the vertical scan axis to create an image of the step position vs time. The dashed curve delineates a single lattice plane. Distortions of that line from the vertical are due to instrument drift. The dotted curve traces out the time evolution of the position of the step. The difference between the two lines gives the fluctuations in average step position. Our estimates of the absolute positions of these two curves are only accurate to ± 1 lattice spacing and show that the fluctuations in step position over this 100 s interval of time are less ≤ ± 1 lattice spacing, with the exception of the time interval between 1 and 3 s, where the deviation from the dashed line is +2 lattice spacings.

Influence of Kink Density on Impurity Pinning — Two Distinct Behaviors. Because of the major influence that impurities have on the growth of mineral surfaces and the extent to which analysis of those effects is used to interpret

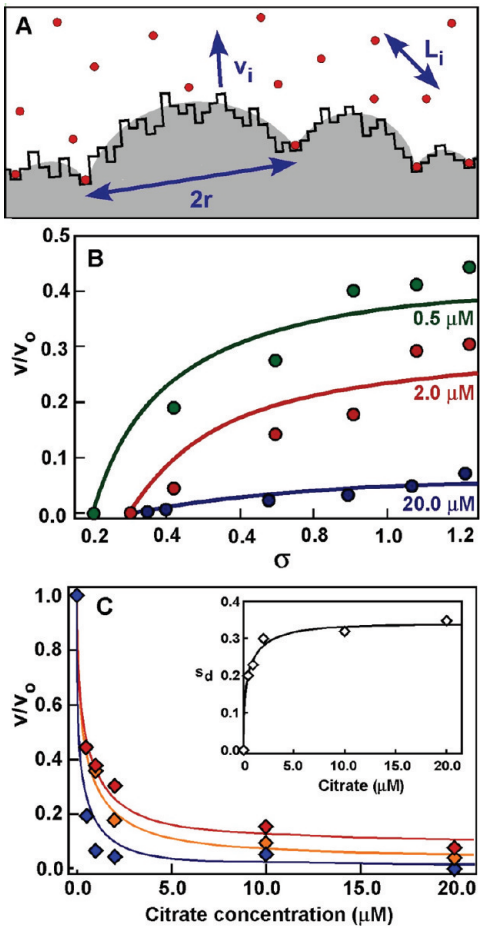

Figure 3. (A) Schematic illustration of step pinning model of Cabrera and Vermilyea[5] showing steps pinned by impurities (red solid circles) where the average impurity spacing is L_i and the critical step radius is r_c. On a microsopic scale, the step consists of may fluctuating kinks, but at the mesoscale, it has an average curvature determined by L_i. Because of the Gibbs−Thomson effect, which gives the reduction in supersaturation brought about by step curvature, the step moves through these impurities with a speed v determined by the ratio of L_i to r_c. (B) Dependence of step speed plotted as v/v_0 vs supersaturation for the [101] step on the ($\bar{1}$01) face of COM growing in the presence of citrate where v_0 is the step speed in pure solution. The curves are fits to the data according to a C−V type model. (C) Dependence of v/v_0 on citrate concentration where the curves are fits to the same model as in (B). The inset shows the width of the dead zone — the region of positive supersaturation where $v = 0$ — vs citrate concentration where the solid curve is a fit to the data of the form expected for adsorption to the terrace. In both (B) and (C), the experimental data are shown for only a few of the curves and the complete data sets can be found in ref 30. Symbols in (C) designate supersaturations of red - 1.2, orange - 1.0, and blue - 0.6.

the conditions in which growth occurred, we now examine how impurities modulate the growth of steps in the rough vs smooth limits. For the case of rough steps, Figure 3a shows the classical representation of inhibition by impurities that adsorb strongly to step edges that arises from the assumption of strong step fluctuations. The origin of this step behavior, inherent to FDT, is governed by the Gibbs−Thomson law, which relates equilibrium concentration to step curvature through:[4,23]

$$C_e(r) = C_e^{\infty} \exp(\omega\gamma/kTr) \qquad (2)$$

where γ is the step edge free energy per unit step length per unit step height, and r is the radius of curvature, and C_e^{∞} designates the equilibrium concentration for the infinitely long, straight step, (i.e., the bulk solubility). As a consequence of eq 2, if step curvature $\Gamma \equiv 1/r$ exceeds the value for which $C_e(r)$ equals or exceeds C itself, the step must stop because it is in thermodynamic equilibrium with the surrounding solution. In other words, at a critical step radius r_c, the local value of C_e equals C.

Cabrera and Vermilyea (CV)[5] recognized that the Gibbs−Thomson relation led to a strong inhibitory effect by impurities capable of binding to a step edge and blocking addition of new growth units. When the spacing between impurities becomes comparable to or less than r_c, the step must come to a complete stop as it tries to bulge between the impurities (Figure 3a). That is, the impurities are said to create a "dead zone" over a superaturation range up to σ_d, where there is no growth even though the solution is supersaturated with respect to the bulk crystal (Figure 3b). The width of the dead zone is defined by the values of $C < C_e(r_c) \equiv C_d$ or, alternatively, by

$$\sigma < \sigma_d \equiv \ln[a_e(r_c)/a_e^{\infty}] \qquad (3)$$

where C_d and σ_d are the concentration and supersaturation up to which no growth occurs and $a_e(r_c)$ and a_e^{∞} are the equilibrium activity products of the solute for the step with critical curvature and the infinitely long, straight step, respectively. Because the average spacing between impurities can be related to the solution impurity concentration, the CV model makes specific predictions about the dependencies of both the step speed and the width of the dead zone on solution impurity concentration.

Calcium oxalate monohydrate (COM) provides a good example of a system that exhibits CV behavior. Citrate poisoning of COM produced the serrated step morphology envisioned in the CV model (Figure 3a) and the predictions of the CV model were in excellent agreement with the measured dependencies of step speed and dead zone width on citrate concentration.[30] As shown in Figure 3b,c, COM shows signature behaviors of systems that fit this model with a rapid drop in step speed at low citrate concentrations that are 100× less than the Ca^{2+} concentration and a dead zone with a width that follows a Langmuir adsorption profile (Figure 3c, inset).

Our results on calcite growth in the presence of Sr^{2+} (Figure 4) exhibit a completely different behavior.[19] As seen in Figure 4b, when plotted versus supersaturation, v shows a step-like rise out of the dead zone to a value that meets or exceeds the step speed of the pure system. In addition, the inset to Figure 4c shows that the relationship between σ_d and C_{Sr} does not exhibit the characteristic CV dependence. In fact, when plotted this way, extrapolation of the data to a zero Sr^{2+} concentration leads to the absurd conclusion that there is a large dead zone even in the absence of Sr! The differences are even more striking when plotted versus impurity concentration (contrast Figure 4c with Figure 3c): At low Sr^{2+} concentrations, calcite step speed remains constant or increases slightly with increasing Sr^{2+} concentration. (This weak increase may be a result of small downward shifts in the solubility constant due to entropy of mixing in the solid, or a slight shift in solute attachment kinetics. The effect is too small and the data too imprecise to differentiate between these sources.) More importantly, above a threshold Sr^{2+} level that meets or exceeds the Ca^{2+} level, the step speed drops precipitously into a dead zone.

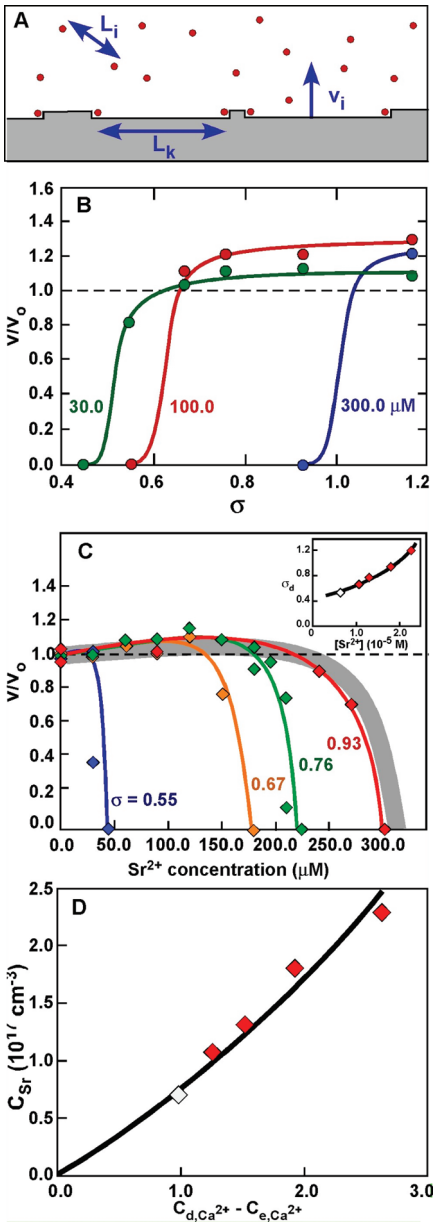

Figure 4. (A) Schematic illustration of step pinning model based on blocking of newly formed kinks by impurities (red solid circles) where the average impurity spacing is L_i and the average kink spacing is L_K. On a microsopic scale, the step consists of extended smooth step-segments bounded by a small number of kinks. The step speed v is hardly affected as long as new kinks can form via one-dimensional (1D) nucleation, but as the rate of kink blocking approaches the rate of creation, the step speed rapidly drops. (B) Dependence of obtuse step speed plotted as v/v_0 vs supersaturation for the calcite (104) face growing in the presence of Sr^{2+} where v_0 is the step speed in pure solution. (C) Dependence of v/v_0 on Sr^{2+} concentration. Dashed line shows the result of introducing a quadratic kink-blocking term to a dependence of step speed on Sr^{2+} concentration that increases linearly with Sr^{2+} concentation as described in the text. The inset shows the width of the dead zone, the region of positive supersaturation where $v = 0$, versus citrate concentration. (D) Dependence of Sr^{2+} concentration where v goes to zero on excess Ca^{2+} concentration. All curves in B–D are guides to the eye. In both (B) and (C), the experimental data are shown for only a few of the curves and the complete data sets can be found in ref 19.

Surprisingly, the dependence seen in Figure 4c was also observed for calcite growth in the presence of aspartic acid (Asp) and Asp-rich peptides containing 2–21 Asp residues, despite the fact that the carboxyl side chains bind directly to the Ca^{2+} ions at the step, whereas Sr^{+} commonly sorbs at mineral surfaces as an outer-sphere surface complex, through relatively weak, electrostatic interactions. Apparently, the mechanism of binding has a minor effect of the mechanism of inhibition.

Propagation of Steps with Low Kink Density. To understand the basis for these dramatically different inhibitory behaviors, we first consider the process by which a step with slow kink fluctuations propagates. In a low kink density situation, the rate-limiting step is no longer attachment of solute molecules to available kinks. Instead, step advance must await the creation of a new kink. Because creation via fluctuations is so slow, new kinks are predominantly created by so-called 1D nucleation (green spheres in Figure 1a). That is, a solute molecule must attach to a fully occupied region of the step edge, thus forming two new kink sites to the left and right (Figures 1a and 4a).[31] This highly unstable configuration must be quickly stabilized by an adjacent attachment event or a detachment event will eliminate the newly formed kink sites before they can propagate. Because solute attachment is fast compared to kink formation in this regime, once formed, these stabilized kinks rapidly spread left and right until they meet other rare kinks moving from right and left or they reach the end of the step segment.[32] In this way, the step propagates forward.

One consequence of this process is that the only way impurities can stop growth is to block the lateral spread of new kinks (Figure 4a). Since each 1D nucleation event creates both a left- and right-facing kink, complete inhibition depends on the probability of two independent impurity attachment events, leading to a nonlinear dependence of the dead zone on impurity concentration. By this process, a higher impurity concentration is required for the onset of inhibition but once active, the inhibiting effect shows a squared or higher order dependence on impurity concentration.

A simple test of this conceptual model shows that we can qualitatively predict the dependencies of both the step speed and dead zone width on impurity concentration. Step advancement stops when the net rates of impurity and solute attachment are equal leading to $C_d - C_e \propto C_i$. As Figure 4d shows, when the experimental results for Sr^{2+} inhibition of calcite are plotted as $(C_d - C_e)$ versus C_{Sr} the result is indeed an approximately linear relationship that correctly extrapolates to zero when $C_{Sr} = 0$. The step speed has two terms that depend on Sr^{2+} level, one that increases linearly with concentration as discussed above, and one that decreases approximately with concentration squared due to the blocking of new kink sites on both the left and right sides. That is, $v \propto (1 + b_1C_i - b_2C_i^2)$ where b_1 and b_2 are independent of impurity concentration. This dependence is illustrated by the gray band in Figure 4c where b_1 and b_2 were chosen to match the initial slope and maximum, respectively. The drop in step speed beyond the maximum is not as precipitous as seen experimentally, but this is to be expected because the quadratic dependence ignores the negative feedback on inhibition inherent to this mechanism. That is, the blocking of one newly created kink pair increases the lifetime of the adjacent kink free regions, increasing the probability that 1D nucleation will eventually occur in that region and thus delaying the drop in speed until a higher concentration where all new kinks can be blocked.

Because step segments in the C−V model are also pinned by two impurity adsorption sites, one might guess that nonlinearity in the dependence of dead zone width on impurity concentration should also be predicted in the rough limit. But the need for independent impurity attachment events emerges in the analysis of kink-limited growth because it is a kinetic model that depends on a comparison of rates (i.e., solute vs impurity attachment). In contrast, the C−V model is based on a thermodynamic analysis, which considers only the ensemble behavior. All that matters in that case is the average impurity spacing vs the critical radius, and that spacing is given by the square root of the areal coverage, which follows a Langmuir dependence on solution impurity concentration.

Simulations of Kink-Limited Growth. Because there is no analytical description of this kink-site limited mechanism of growth and inhibition, we used kinetic Monte Carlo (kMC) simulations to test its ability to reproduce experimental observations and to provide insights into the governing parameters. We simulated step-mediated crystal growth with a simple solid-on-solid surface model. The solution phase was represented by an infinite reservoir of solvent molecules and impurities that impinged on the crystal surface at a constant rate. We assumed fast diffusion in the solution phase, thus providing uniform concentrations (and impingement rates) at the growing surface. Our simulations modeled the effect of the basic physical events: attachment and detachment of solute and impurities at the crystal surface. While attachment events included adsorption of both growth units and impurities on the growing crystal surface, detachment events included desorption of growth units only in order to capture the behavior of the system for strongly binding impurities. For the results presented here, impurities were assumed to be incorporated in the crystal rather than desorb back into solution. The role of surface diffusion during solution growth is somewhat controversial, and for simplicity we do not show the results of simulations that include this process. Thus, the kMC model represents the time evolution of the system resulting from the random execution of these two events with rates selected according to the local environment. Impurities are included in the flux from the solution and their effect is simply to reduce the binding energies of growth units on neighboring sites. Other details of the simulations, such as definition of attachment and detachment probabilities and the consequence of finite impurity lifetimes are given in Appendix A.

Using this model, we tracked the evolution of surface steps and studied their behavior as a function of supersaturation and impurity concentration. Typical snapshots in time from the kMC simulations show why impurity interactions are different when kinks are rare (Figure 4a−d). Using the value of one-half 0.225 eV for the nearest neighbor bond strength [33] (twice the kink formation energy), these kMC simulations predict the average kink spacing at equilibrium is ~30 lattice sites (Figure 5a). When an excess solute concentration, which defines the net flux to the step edge, is imposed upon the system, the step advances by 1D nucleation and spread of new kinks at a rate that is proportional to this excess. When the system is further modified by introducing impurities that irreversibly bind to the step, it continues to propagate at full speed (Figure 5b,c) as long as growth units can still attach along at least one kink direction to supply new step edge with unblocked nuclei. When the impurity concentration reaches

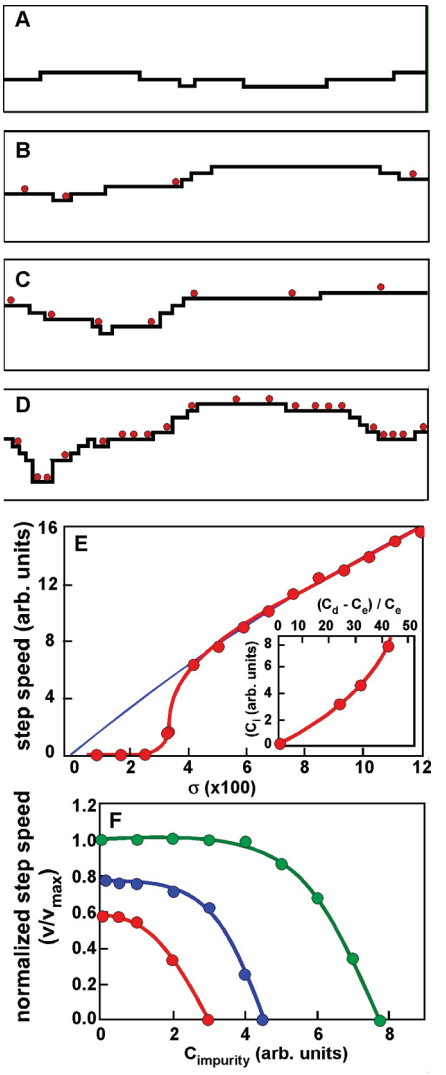

Figure 5. (A−D) Results of kinetic Monte Carlo simulations showing evolution of step with high kink formation energy (low kink density) due to blocking of kinks by adsorption of impurities (solid red circles). Step configurations are snapshots in time from a single simulation. Step is completely stopped in (D). (E) Predicted dependence of step speed on supersaturation derived from the simulations. Inset shows predicted dependence of impurity concentration at which step speed goes to zero vs relative supersaturation (excess solute concentration divided by equilibrium concentration). (F) Predicted dependence of step speed on impurity concentration. Here, in order to separate the curves for clarity, the step speed has been normalized by a single step speed, that is, the maximum step speed for the curve obtained at the highest supersaturation (σ = 0.41) with no impurities.

the level where all new kinks are blocked either at creation or during propagation, the step stops (Figure 5d).

The simulation clearly shows that a blocked step does not exhibit regions of critical curvature between pinning sites. That is, impurities are not halting growth by the Gibbs−Thomson rule that inhibition occurs when $L_i < 2r_c$. Rather, impurities stop the step by blocking sites of additional solute attachment, that is, the kinks. By running these simulations for varying fluxes of solute and impurity molecules, we extracted the predicted dependencies of step speed and dead zone on impurity concentration. As Figure 5e,f shows, the results are similar to the experimental observations for Sr^{2+} inhibition of calcite (compare with

Figure 4b,c) and in strong contradiction to the predictions based on the Gibbs−Thomson law (compare with Figure 3b,c). As in the calcite-Sr system the step speed jumps from zero to the uninhibited speed as supersaturation is increased by a factor of 1.3−1.5 (Figures 4b and 5e), while for the COM-citrate case it never recovers to its full speed and requires a factor of 4 increase to approach the limiting v/v_0 (Figure 3b).

The simulation also shows C_i scales slightly nonlinearly with $C_d - C_e$ (Figure 5e inset) as for calcite with Sr^{2+} (compare with Figure 4d) and does not exhibit the characteristic behavior expected from the C−V model (compare with Figure 3c inset). Thus, despite the simplicity of this model, the qualitative behavior of the experiments is well captured, supporting the argument for a description of growth and inhibition based on weak step fluctuations.

The results presented here are for impurities that never desorb. Clearly, the nature of impurity binding should impact the details of the dependence of step speed on supersaturation. Indeed, in other sets of simulations for which the impurity lifetime is finite, the details of the dependence vary with shorter lifetimes and result in a less sharp rise from the dead zone. But these are secondary effects. In all cases, the dependence never takes on the form observed for COM with citrate or predicted by C−V type models. The observed mechanism of inhibition is through blocking of the kinks and step advancement is not arrested until all kinks are all blocked.

The results of these simulations can be compared with those of van Enckevort and van den Berg[34] and van Enckevort and Los.[35] In those studies, values of the kink formation energy were chosen such that the steps were in one of two regimes. In the first, the crystal was thermally roughened so that the step edge energy was zero and there was no limit to the step curvature possible at any value of σ. In the second, the bond energies were chosen such that the crystal was slightly below the roughening transition (nearest neighbor bond energy $\sim 1-2\ kT$). The first case is not relevant the situation considered here. Even in the second case, at the lower end of the energy range, growth transitioned from step flow to 2D nucleation at very low supersaturations and thus are not comparable to the systems considered here. However, at the higher end of the energy range, growth proceeded by step flow and, as supersaturation was increased, the presence of impurities led to a dead zone followed by recovery. Moreover, the predictions of the C−V model were largely obtained, both in terms of the dependence of step speed on supersaturation and the width of the dead zone on impurity concentration. As a result, the dependencies observed there are similar to those obtained experimentally in the COM-citrate system. (Compare Figure 5 of ref 30 to Figure 6 of ref 34.) The simulation results presented here are for larger bond energies where kink densities are low. Consequently, when the two sets of simulation results are combined, the complete range of behavior observed in the experiments can be understood in terms of the rates of attachment and detachment events.

Implications

The kink-limited condition is likely to apply to a broad range of low solubility minerals with both geological and biological significance. This is because the underlying source of differences between systems that display classic growth behavior and those that display kink-limited characteristics is the energy barrier to forming a new kink by thermally activated exchange between crystal and solution. When this barrier is high compared to kT, fluctuations will be weak and kink formation will be slow. Following the rule of thumb for chemical kinetics, this high barrier should imply large bond strength between adjacent molecules along the step edge so that, even at equilibrium, kink densities will also be low. But since the solubility of a crystal is also largely determined by thermal detachment probabilities, this condition should generally hold for sparingly soluble crystals. Because low solubility is a requirement for stability in dilute aqueous systems, our findings are likely to be applicable to many different minerals prevalent in near-surface earth environments. Indeed, in addition to the calcium carbonates, calcium phosphates and silicate minerals play key roles in near-surface geochemical and biological environments and also fulfill important technological roles.

The realization that a kink-limited description is required to understand how impurities interact with sparingly soluble materials during growth has a number of broad implications. Over the past 50 years, the interactions of trace and minor elements with calcium carbonate minerals have become a central focus of efforts to understand the interplay between earth materials and biota through time. In particular, the impurity contents or signatures in marine cements[36,37] and calcified skeletal structures[38−40] are the basis for long-standing (and emerging) proxy models that reconstruct the temperature[41−44] and seawater chemistry of past environments.[38,40,45] These composition-based models assume that signatures reflect the physical and chemical conditions of mineralization, but in many situations, the impurity levels in inorganic and biotic carbonate minerals alike show significant departures from expected equilibrium values.[39,40,45,46] A recent in vitro investigation found that just the presence of peptides in growth solutions enhanced Mg levels by an amount equivalent to what would be expected for an increase in growth temperature of several degrees,[47] suggesting that vital effects can arise from purely physiochemical mechanisms. Studies using high-resolution in situ approaches have provided some insights by showing why similar impurities such as strontium[19] and magnesium[20,21] have distinctly different influences on calcite growth, and others have hinted at the importance protein−solvent interactions in altering the basic atomistic dynamics of crystal surfaces.[22,48] Yet, a complete mechanistic picture for the origins of these effects has remained elusive.

Related studies show that the trace element contents in calcite generally appear to be in "kinetic disequilibrium" from their corresponding growth solutions. That is, faster growth rates increase the uptake of trace and minor elements,[21,49−51] and the impurity signatures are dependent upon step edge direction[21,51] to give sector zoning—the macroscopic result of differential uptake.[49,50] One recent study explained these effects by an "entrapment efficiency" model, a conceptual construct related to near-surface impurity diffusivity and surface layer thickness.[52] But this mass transport-dependent view of impurity incorporation is at odds with the conclusions of the study on peptide enhancement of Mg levels discussed above.[47] These same peptides were also shown to accelerate growth rates by reducing the activation barrier to solute attachment at steps.[22] These results suggest that the atomistic kinetics of impurity- and solvent-step interactions outweigh factors associated with mass-transport in controlling impurity

incorporation. Indeed, the findings reported here lead us to suggest an alternative, kinetics-based picture of differential uptake: Increasing the supersaturation (growth rate) increases the probability (density) of 1D nucleation events along the otherwise kink-poor step edge, thus creating more opportunities for impurity binding and incorporation. This mechanism also naturally leads to a dependence on step direction since the energetics of kink creation at distinct step edges will differ. Furthermore, this suggests a physical basis for why greater growth temperature correlates with higher impurity signatures: by ratcheting up thermal creation of kinks, the probability of impurity binding and incorporation is increased.

Other situations in which the findings reported here have significant implications include both functional and pathological tissue mineralization, low-temperature aqueous deposition of silicates, and growth of protein crystals. Looking beyond the implications for these traditional aqueous systems, growth and coarsening of nanocrystals or nanowires should also occur in a kink-limited regime. Evidence for this comes from analysis of island coarsening on GaAs,[53] where the GTL was found to be inadequate to explain coarsening rates. Here the need for a theory of weak fluctuations arises not from inherent properties of the material, but rather from the system size itself. The recent discovery that faceted nanowires growing from solution advance on steps generated at screw dislocations[54] serves to highlight the links to the findings presented here. More generally, except in cases where a step is atomically rough, one can always define a system size that falls below that average spacing between fluctuations for a given time scale. This statement should also apply to other types of fluctuations in nanoscale systems, including those that eliminate thermodynamic imbalances caused by voltage differences, stresses, or temperature gradients. The implication is that nanoscale systems in general, not just those involving crystallization, require a theory of weak fluctuations to describe their behavior. Describing crystal growth of weakly fluctuating steps should provide a start.

Acknowledgment. The authors acknowledge D.S. Wilson and M.L Weaver for collecting AFM data on Sr^{2+} inhibition of calcite and citrate inhibition of calcium oxalate, respectively. They also thank the anonymous reviewers for extensive comments that greatly improved the manuscript. This work was supported by awards to JDY performed under the auspices of the U.S. Department of Energy by Lawrence Livermore National Laboratory under Contract DEAC52-07NA27344 (high resolution AFM on calcite), grant DK61673 from the National Institutes of Health (AFM results on COM), and at the Molecular Foundry, Lawrence Berkeley National Laboratory, with support from the Office of Science, Office of Basic Energy Sciences, of the U.S. Department of Energy under Contract No. DE-AC02-05CH11231 (Concepts and theoretical analysis). Support for LAZR, AC and GG was provided by the Laboratory Directed Research and Development Office at Lawrence Livermore National Laboratory (kinetic Monte Carlo simulations and analysis). This work was also supported by awards to PMD by Department of Energy FG02-00ER15112 (concepts and AFM results on Sr^{2+}-calcite), National Science Foundation OCE-052667 (concepts, AFM data on Sr^{2+}-calcite, analysis) and the National Science Foundation EAR-0545166.

Appendix A

Our KMC algorithm is as follows. Starting from a given initial configuration, all mobile particles on the surface are placed in different lists based on their number of neighbors (n). In the case of a Kossel crystal, there are only six lists. Attachment and detachment rates are defined as

$$R^{+} = \nu \exp[-E_3/kT] \text{ (attachment)} \quad \text{(A1a)}$$

$$R^{-}{}_{n} = \nu \exp[-E_n/kT] \text{ (detachment)} \quad \text{(A1b)}$$

where ν is frequency, and E_n is the energy of a particle with n neighbors. The attachment rate is given by a constant driving force, which is equal to the energy of a particle at a kink site (i.e., three neighbors) and the detachment rate depends on local environment (i.e., number of neighbors: n).

In our model, an impurity "blocks" a site by reducing the number of "effective" neighbors to a solute particle. This way, a solute molecule next to an impurity had a higher probability of detachment than one next to another solute molecule. For example, a solute particle with two regular neighbors and 1 impurity neighbor, will have an energy $E = E_2$ because, although it has three neighbors, one of them is an impurity.

Rates for impurities are defined as

$$R^{+}{}_{i} = f^{+}R^{+} \quad \text{(A2a)}$$

$$R^{-}{}_{i} = f^{-}R^{-} \quad \text{(A2b)}$$

where f^{+} and f^{-} are factors to obtain the desired impurity concentration.

The total rate is the sum of all individual rates weighted by the number of particles (both solute and impurities) in each energy environment:

$$R_{\text{total}} = \Sigma(M_n R^{-}{}_{n} + S_n R^{+}) \quad \text{(A3)}$$

where M_n and S_n are the number of particles with n neighbors and the number of vacant sites at the surface with n neighbors, respectively (a particle landing in a vacant surface site in which there are n neighbors is S_n).

Therefore, the probability of each event is given by the ratio of the individual event rate to the total rate:

$$P^{+}{}_{n} = (S_n R^{+})/R_{\text{total}}$$

$$P^{-}{}_{n} = (M_n R^{-})/R_{\text{total}}$$

For completeness, although impurity detachment is also dependent on number of neighbors, in the case presented here we chose it to be $R^{-}{}_{i} = 0$ and therefore the detachment probability of an impurity is also 0. By varying the values of f^{+} and f^{-}, we also analyzed a range of impurity lifetimes, as discussed below.

The surface consisted of a three-dimensional cubic grid, 300×300 units in the lateral dimensions, and containing a single unit height step. Periodic boundary conditions were used in the simulations with a vertical displacement of one step height between the two sides of the computational cell. Solute and impurity molecules impinged upon random sites on the surface at a constant rate. Detachment probabilities of both solute and impurity molecules was based solely on the number of neighbors (as defined above). In order to accelerate the simulations, the probabilities of attachment and detachment to and from flat terrace sites were reduced by a factor of 10^{-4} (to preserve microscopic reversibility).

Attachment and detachment rates for the solute molecules were fixed by the choice of bond strengths and impurity attachment and detachment rates were varied over a wide range. Results are shown here only for impurities that bind preferentially to steps and have an infinite lifetime at the step

edge. The kinetic barrier to creation of a kink by detachment from the step edge was set at 0.225 eV and the system was allowed to evolve for 10^8 time steps. The predicted dependencies of step speed on impurity concentration and supersaturation were then obtained by analyzing a series of runs over a range of solute and impurity fluxes.

Rather than attempting to produce a calcite-specific model in which all processes and associated energy barriers are correctly included, which would be impossible, given the current state of knowledge concerning both, the goal of these simulations was to test whether a system with bond strengths consistent with those of calcite and other sparingly soluble minerals reproduced the kinds of step morphologies and impurity effects seen in experiments. To illustrate the findings, we believe that choosing the simplest of models — impurities bind to steps and stay there — is the most useful. In fact, a range of impurity lifetimes were examined in our simulations. These were modeled by varying impurity desorption rates from values equivalent to solute detachment rates to no detachment at all. The latter corresponds to the case of infinite lifetime reported in this manuscript. However, similar effects on the reduction of step velocity were obtained for impurities that were allowed to desorb. The lower the lifetime of the impurity, the higher the impurity concentration needed to fully stop the motion of the step, but in all cases, as long as $\varepsilon \gg kT$, the behavior was qualitatively similar. Finally, when using values of $\varepsilon \sim kT$ we recover the behavior of high kink density, a regime that has been well explored by others through kMC simulations.[34,35] The full set of results will be published in a separate paper.

Note Added after ASAP Publication. This paper was posted on November 11, 2009, before all the corrections were incorporated. A new corrected version was posted on November 13, 2009.

References

(1) Burton, W. K.; Carbrera, N.; Frank, F. C. *Royal Soc. London Philos. Trans.* **1951**, *A243*, 299.

(2) Strictly speaking, this is only true for the class of crystals known as Kossel crystals. In systems where a complete growth unit has multiple subunits, the attachment or detachment of all subunits is required to leave the chemical potential unchanged.

(3) Reif, F. *Fundamentals of Statistical and Thermal Physics*; McGraw-Hill: San Francisco, 1965; pp 572−573.

(4) Gibbs, J. W. *Trans. Connect. Acad. Sci.* **1876**, *3*, 108. Gibbs, J. W. *Trans. Connect. Acad. Sci.* **1878**, *16*, 343.

(5) Cabrera, N.; Vermilyea, D.A. In *Growth and Perfection of Crystals; Proceedings*; Doremus, R. H., Roberts, B. W., Turnbull, D., Eds.; Wiley: New York, 1958; p 393.

(6) Yau, S.-T.; Thomas, B. R.; Vekilov, P. G. *Phys. Rev. Lett.* **2000**, *85*, 353–356.

(7) Yau, S.-T.; Petsev, D. N.; Thomas, B. R.; Vekilov, P. G. *J. Mol. Biol.* **2000**, *303*, 667.

(8) The opposite limit of weak step fluctuations, also follows from the BCF theory when the kink energy is large as compared to the thermal energy (Voronkov, V. V. *Sov. Phys. Crystallography*, **1970**, *15*, 8; 1972, 18, 19). However, the option of weak fluctuations, that is, of low kink density, was not explored, partly due to lack of experiments and partly because of the standard concept that one dimensional (1D) systems, like steps, are always strongly fluctuating. In other words, the step should always have high kink density. The latter statement, similar to FDT, is indeed correct, but only when the 1D object is sufficiently long and/or is observed over a long period of time. The latter temporal limitation, away from equilibrium, requires not only low kink energy, but also low attachment/detachment kinetic constants. With this distinction, we want to differentiate our use of the word rough as a measure of high kink density determined by the kinetics of thermal step fluctuations from its use in the thermodynamic sense of a "thermal roughening transition", where the step edge energy vanishes.

(9) Burton, W. K.; Cabrera, N. *Disc. Faraday Soc.* **1949**, *5*, 33–39.

(10) Qin, X. R.; Lagally, M. G. *Science* **1997**, *278*, 1444.

(11) Zhang, J.; Nancollas, G. H. *J. Cryst. Growth* **1990**, *106*, 181.

(12) Chernov, A. A. *J. Cryst. Growth* **2004**, *264*, 499.

(13) Nielsen, A. E. *Pure Appl. Chem.* **1981**, *53*, 2025.

(14) Cuppen, H. M.; Meekes, H.; van Veenendaal, E.; van Enckevort, W. J. P.; Bennema, P.; Reedijk, M. F.; Arsic, J.; Vlieg, E. *Surf. Sci.* **2002**, *506*, 183.

(15) Cuppen, H. M.; Meekes, H.; van Enckevort, W. J. P.; Vlieg, E. *Surf. Sci.* **2004**, *571*, 41–62.

(16) Chernov, A. A.; Rashkovich, L. N.; Yamlinski, I. V.; Gvozdev, N. V. *J. Phys.: Condens. Matter* **1999**, *11*, 9969.

(17) Chernov, A. A.; De Yoreo, J. J.; Rashkovich, L. N.; Vekilov, P. G. *Mater. Res. Soc. Bull* **2004**, *29*, 927.

(18) Georgiou, D. K.; Vekilov, P. G. *Proc. Natl. Acad. Sci. U. S. A.* **2006**, *103*, 1681.

(19) Wasylenki, L. E.; Dove, P. M.; Wilson, D. S.; De Yoreo, J. J. *Geochim. Cosmochim. Acta* **2005**, *69*, 3017.

(20) Davis, K. J.; Dove, P. M.; De Yoreo, J. J. *Science* **2000**, *290*, 1134–1137.

(21) Wasylenki, L. E.; Dove, P. M.; De Yoreo, J. J. *Geochim. Cosmochim. Acta* **2005**, *69*, 4227.

(22) Elhadj, S.; De Yoreo, J. J.; Hoyer, J. R.; Dove, P. M. *Proc. Natl. Acad. Sci. U. S. A.* **2006**, *51*, 19237.

(23) Teng, H. H.; Dove, P. M.; Orme, C. A.; De Yoreo, J. J. *Science* **1998**, *282*, 724.

(24) Teng, H. H.; Dove, P. M.; De Yoreo, J. J. *Geochim. Cosmochim. Acta* **2000**, *64*, 2255.

(25) Higgins, S. R.; Bosbach, D.; Eggleston, C. M.; Knauss, K. G. *J. Phys. Chem. B* **2000**, *104*, 6978.

(26) Christoffersen, J; Rostrup, E; Christoffersen, M. R. *J. Cryst. Growth* **1991**, *113*, 599.

(27) Rashkovich, L. N.; Mkrtchyan, A. A.; Chernov, A. A. *Sov. Phys. Crystallogr* **1985**, 30.

(28) Thomas, T. N.; Land, T. A.; Martin, T.; Casey, W. H.; De Yoreo, J. J. *J. Cryst. Growth* **2004**, *260*, 566.

(29) Rashkovich, L. N.; Shustin, O. A.; Chernevich, T. G. *Phys. Sol. State* **2000**, *42*, 1921.

(30) Weaver, M. L.; Qiu, S. R.; Hoyer, J. H.; Nancollas, G. H.; Casey, W. H.; De Yoreo, J. J. *J. Cryst. Growth* **2007**, *306*, 135.

(31) In the simple case of a cubic lattice, this first molecule binds to the crystal through two bonds, one with the terrace and one with the step edge. Therefore, not only is it weakly bound, its chemical potential is equal to that of the solution rather than the crystal. Because it is so weakly bound to the step — as compared to a molecule in a true kink position where it has three saturated bonds with the lattice — it will detach after a short time, unless it is stabilized by attachment of another molecule to the step on either its immediate left or right. As soon as this happens, each of the molecules in this newly created pair is in a true kink position and thus acquires the chemical potential of the crystal (to the first nearest neighbor approximation) (Figures 1a and 4a).

(32) Of course, even the stabilized 1D nucleus has some probability of disappearing by sequential detachment of both molecules. However, the frequency of this event is much lower than for the lone molecule because of the added bond. In a supersaturated solution, the average attachment frequency to the new kink-pair exceeds that of detachment, so there is a nonzero probability that this pair will survive and stay forever, thus giving rise to a new molecular row.

(33) No direct measurements of kink energies for calcite exist, but estimates based on either heats of dissolution or modeling give values close to 0.25eV (nearest neighbor bond values close to 0.25eV). See, for example, de Leeuw, N. H.; Parker, S. C.; Harding, J. H. *Phys. Rev. B* **1999**, *60*, 13792.

(34) van Enckevort, W. J. P.; van den Berg, A. C. J. F. *J. Cryst. Growth* **1998**, *183*, 441–455.

(35) van Enckevort, W. J. P.; Los, J. H. *J. Phys. Chem. C* **2008**, *112*, 6380–6389.

(36) Berner, R. A.; Westrich, J. T.; Graber, R.; Smith, J.; Martens, C. S. *Am. J. Sci.* **1978**, *278*, 816.

(37) Carter, P. W.; Mitterer, R. M. *Geochim. Cosmochim. Acta* **1978**, *42*, 1231.

(38) Elderfield, H.; Ganssen, G. *Nature* **2000**, *405*, 442.

(39) Bentov, S.; Erez, J. *Geochem. Geophys. Geosyst.* **2006**, *7*, Q01P08.

(40) Dickson, J. A. D. *Science* **2002**, *298*, 1222.

(41) Nurnberg, D.; Bijma, J.; Hemleben, C. *Geochim. Cosmochim. Acta* **1996**, *63*, 2369.
(42) Rosenthal, Y.; Boyle, E. A.; Slowey, N. *Geochim. Cosmochim. Acta* **1997**, *61*, 3633.
(43) Lear, C. H.; Elderfield, H.; Wilson, P. A. *Science* **2000**, *287*, 269.
(44) Anand, P.; Elderfield, H.; Conte, M. H. *Paleoceanography* **2003**, *18*, 1.
(45) Lea, D.W. In Elderfield, H. *The Oceans and Marine Geochemistry*; Elsevier: New York, 2006; p 365.
(46) Weiner, S.; Dove, P. M. *Rev. Mineral. Geochem.* **2003**, *54*, 1.
(47) Stephenson, A. E.; DeYoreo, J. J.; Wu, L.; Wu, K. J.; Hoyer, J. R.; Dove, P. M. *Science* **2008**, *322*, 724.
(48) Elhadj, S.; Salter, A.; Wierzbicki, A.; De Yoreo, J. J.; Dove, P. M. *Cryst. Growth Des.* **2006**, *6*, 197.
(49) Paquette, J.; Reeder, R. J. *Geochim. Cosmochim. Acta* **1995**, *59*, 735.
(50) Reeder, R. J. *Geochim. Cosmochim. Acta* **1996**, *60*, 1543.
(51) Davis, K. J.; Dove, P. M.; Wasylenki, L. E.; De Yoreo, J. J. *Am. Mineral.* **2004**, *89*, 714.
(52) Watson, E. B. *Geochim. Cosmochim. Acta* **2004**, *68*, 1473.
(53) Kaganer, V. M.; Ploog, K. M. *Phys. Rev. B* **2006**, *73*, 115425.
(54) Bierman, M. J.; Lau, Y. K. A.; Kvit, A. V.; Schmitt, A. L.; Jin, S. *Science* **2008**, *320*, 1060.